Optical Engineering

OpticalEngineering.SPIEDigitalLibrary.org

Modified tandem gratings anastigmatic imaging spectrometer with oblique incidence for spectral broadband

Chengguang Cui
Shurong Wang
Yu Huang
Qingsheng Xue
Bo Li
Lei Yu

SPIE.

Downloaded From: http://opticalengineering.spiedigitallibrary.org/ on 05/29/2016 Terms of Use: http://spiedigitallibrary.org/ss/TermsOfUse.aspx

Modified tandem gratings anastigmatic imaging spectrometer with oblique incidence for spectral broadband

Chengguang Cui,[a,b] Shurong Wang,[a,*] Yu Huang,[a] Qingsheng Xue,[a] Bo Li,[a] and Lei Yu[a]
[a]Chinese Academy of Sciences, Changchun Institute of Optics, Fine Mechanics and Physics, Changchun 130033, China
[b]University of Chinese Academy of Sciences, Beijing 100049, China

Abstract. A modified spectrometer with tandem gratings that exhibits high spectral resolution and imaging quality for solar observation, monitoring, and understanding of coastal ocean processes is presented in this study. Spectral broadband anastigmatic imaging condition, spectral resolution, and initial optical structure are obtained based on geometric aberration theory. Compared with conventional tandem gratings spectrometers, this modified design permits flexibility in selecting gratings. A detailed discussion of the optical design and optical performance of an ultraviolet spectrometer with tandem gratings is also included to explain the advantage of oblique incidence for spectral broadband. © *2015 Society of Photo-Optical Instrumentation Engineers (SPIE)* [DOI: 10.1117/1.OE.54.9.095104]

Keywords: tandem gratings; anastigmatic; imaging spectrometer; optical system design.

Paper 150796 received Jun. 13, 2015; accepted for publication Sep. 3, 2015; published online Sep. 30, 2015.

1 Introduction

Imaging spectrometers with reflection gratings are widely used in ultraviolet (UV) scientific research and engineering applications.[1,2] These spectrometers are used in atmospheric sounding and ocean optics, as well as studying the spatially resolved ultrashort pulse characterization.[3–5] At present, several related fields are showing increasing attention to the requirements of imaging spectrometers with high spectral resolution. Astigmatism, which is the primary aberration of some imaging spectrometers, such as Czerny–Turner and Ebert–Fastie imaging spectrometers, has been investigated in the past years.[6,7] Spectrometers with one or more anastigmatic wavelengths have been proposed for different applications. Czerny–Turner and Ebert–Fastie spectrometers with 1-wavelength anastigmatic, as well as Offner and Dyson spectrometers with 2-wavelength anastigmatic have been designed and extensively used in the field of solar observation.[8,9] However, the disadvantage of these designs above is that the stigmatic image can be obtained only for some selected wavelengths.

To reduce astigmatism over a large wavelength region, Bartoe and Brueckner provided a large-scale imaging spectrometer with tandem gratings and Wadsworth mounting for coaxial telescope applications.[10] In their design, 2 gratings were located to be tangent to the circle of the radius of the concave grating. The central light from the fore-optics was the normal incident on this spectrometer. Yu and Lin presented a small-scale imaging spectrometer with tandem gratings for both off-axis and coaxial telescope applications.[11] In their design, the former plane grating was located on the Rowland circle of the latter curve grating, and the ruling densities of the gratings were identical. In the present work, a modified large-scale spectrometer with tandem gratings and oblique incidence is developed. This design satisfies astigmatism-corrected conditions in spectral broadband. Compared with conventional tandem gratings imaging spectrometers, the modified design is proposed to determine anastigmatic condition and initial optical structure.

The modified tandem gratings imaging spectrometer has different ruling densities, and astigmatism removal is analyzed based on the geometric aberration theory and Wadsworth condition. The light from the fore-optics is oblique incident on the former grating of tandem gratings spectrometer in our design, which permits flexibility in selecting the types of gratings. The proposed spectrometer exhibits significant potential for a wide range of applications. The grating of tandem gratings spectrometer is not sensitive to polarization of the incoming light, as the angles of incidence are quite small in our design.

2 Anastigmatic Condition and Spectral Resolution

Satisfying astigmatism-corrected conditions in spectral broadband for conventional tandem gratings imaging spectrometers is difficult. The subsequent discussion focuses on astigmatism, which is the primary aberration of imaging spectrometers. The mounting of the tandem gratings is shown in Fig. 1.

According to the theory of concave grating,[12] the meridian and sagittal focal distances can be expressed as

$$\begin{cases} r_m = \cos^2\theta / [R^{-1}(\cos i + \cos\theta) - r^{-1}\cos^2 i] \\ r_s = 1/[R^{-1}(\cos i + \cos\theta) - r^{-1}] \end{cases}. \quad (1)$$

The incident light is parallel to the plane grating G_1 and the radius r of G_1 is infinite; thus, r_m and r_s are also infinite, as shown in Fig. 1. Therefore, the object distance of the concave grating G_2 is infinite according to Eq. (1). The difference between the meridian and sagittal focal distances by mirror can be expressed as

*Address all correspondence to: Shurong Wang; E-mail: 2736517057@qq.com

0091-3286/2015/$25.00 © 2015 SPIE

Downloaded From: http://opticalengineering.spiedigitallibrary.org/ on 05/29/2016 Terms of Use: http://spiedigitallibrary.org/ss/TermsOfUse.aspx

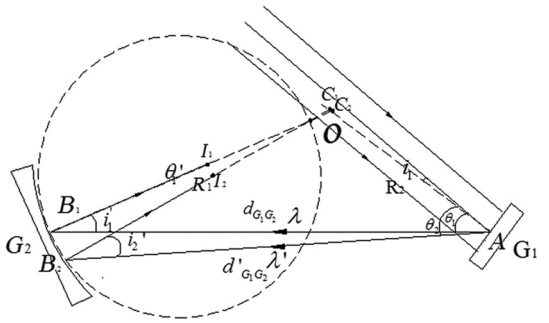

Fig. 1 Mounting of tandem gratings. G_1 is the plane grating. G_2 is the concave grating with radius R_1. i_1 and θ_1 are the first incidence and diffraction angles of G_1. i_1' and θ_1' are the corresponding angles for G_2. I_1 and I_2 denote the image positions at different wavelengths. The ruling densities of G_1 and G_2 are different. θ_2 is the diffraction angle of G_1, and i_2' is the corresponding incident angle of G_2. $d_{G_1G_2}$ and $d'_{G_1G_2}$ are the distances between G_1 and G_2 at different wavelengths.

$$\delta = r_s - r_m = R_2 \sin^2\theta'(\cos\, i' + \cos\,\theta')^{-1}. \tag{2}$$

The astigmatism will be corrected if $\theta' = 0$, which is the optimal Wadsworth condition. The optimum focal distance is:

$$r = R_2(1 + \cos\, i')^{-1}. \tag{3}$$

The incident angle i' of G_2 is modified because of the diffraction of G_1. Therefore, the proper positions of the gratings should be considered to satisfy astigmatism correction for the working waveband.

The geometric relationship of triangles AB_1C_1 and AB_2C_2 is shown in Eq. (4):

$$\begin{cases} 0 = d_{G_1G_2}^2 + B_1C_1^2 - AC_1^2 - 2d_{G_1G_2}B_1C_1\,\cos\, i_1' \\ 0 = d_{G_1G_2}'^2 + B_2C_2^2 - AC_2^2 - 2d'_{G_1G_2}B_2C_2\,\cos\, i_2' \end{cases}. \tag{4}$$

Given that AB_2I_2 is similar to AB_1I_1 for λ', we will only discuss AB_1I_1. In this case, AC_1 can be expressed as $AC_1 = B_1C_1\sin^{-1}\theta_1\,\sin\, i_1'$. In triangle AB_1C_1,

$$\begin{aligned} 0 = {} & d_{G_1G_2}^2 + B_1C_1^2 - (B_1C_1\sin^{-1}\theta_1\,\sin\, i_1')^2 \\ & - 2d_{G_1G_2}B_1C_1\,\cos\, i_1'. \end{aligned} \tag{5}$$

The differential of Eq. (5) with respect to θ_1 is then equal to zero. It is differentiated with respect to θ_1 and the resulting evaluated expression is

$$\begin{aligned} 0 = {} & B_1C_1\frac{\partial B_1C_1}{\partial\theta_1} + d_{G_1G_2}\frac{\partial d_{G_1G_2}}{\partial\theta_1} - d_{G_1G_2}\,\cos\, i_1'\frac{\partial B_1C_1}{\partial\theta_1} \\ & - B_1C_1\,\cos\, i_1'\frac{\partial d_{G_1G_2}}{\partial\theta_1} + d_{G_1G_2}B_1C_1\,\sin\, i_1'\frac{\partial i_1'}{\partial\theta_1} \\ & - \sin^{-4}\theta_1[B_1C_1^2\sin^2 i_1'\,\sin\,\theta_1\,\cos\,\theta_1 \\ & - \left(B_1C_1\sin^2 i_1'\frac{\partial B_1C_1}{\partial\theta_1}\right. \\ & \left. + B_1C_1^2\,\sin\, i_1'\,\cos\, i_1'\frac{\partial i_1'}{\partial\theta_1}\right)\sin^2\theta_1]. \end{aligned} \tag{6}$$

To determine the distance between G_1 and G_2, Eq. (6) should be simplified. Yu and Lin provided a solution when

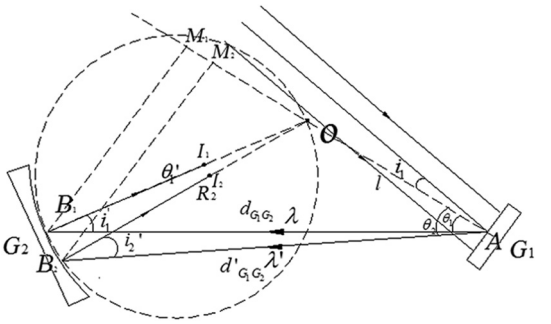

Fig. 2 Modified spectrometer with tandem gratings.

$\partial i_1'/\partial\theta_1 = 0$. In our design, we expect $\partial B_1C_1/\partial\theta_1 = 0$, that is, scalar B_1C_1 is independent of θ_1. If $\partial B_1C_1/\partial\theta_1 = 0$, we obtain the anastigmatic condition for the spectral broadband. As the light bundle of each wavelength will be diffracted in the first order by G_2 along the local normal of its cross section, the extended diffracted light bundle will be intersected at O. When C is located at O, $\partial B_1C_1/\partial\theta_1 = 0$, i.e., $B_1C_1 = R_1$ and O located at the local normal of the relative section of G_1, i.e., $AC_1 = l$, as shown in Fig. 2. Then the evaluated expression is

$$\begin{aligned} 0 = {} & (d_{G_1G_2} - R_2\,\cos\, i_1')\frac{\partial d_{G_1G_2}}{\partial\theta_1} + d_{G_1G_2}R_2\,\sin\, i_1'\frac{\partial i_1'}{\partial\theta_1} \\ & - \sin^{-4}\theta_1\left[R_2^2\sin^2 i_1'\,\sin\,\theta_1\,\cos\,\theta_1\right. \\ & \left. - R_2^2\sin^2\theta_1\,\sin\, i_1'\,\cos\, i_1'\frac{\partial i_1'}{\partial\theta_1}\right], \end{aligned} \tag{7}$$

$$l\sin^{-1} i_1' = R_2\sin^{-1}\theta_1. \tag{8}$$

By differentiating Eq. (8) with respect to θ_1 and the evaluated expression is

$$\frac{\partial i_1'}{\partial\theta_1} = \frac{l\,\cos\,\theta_1}{R_2\,\cos\, i_1'}. \tag{9}$$

Therefore, Eq. (7) can be expressed as follows:

$$(d_{G_1G_2} - R_2\,\cos\, i_1')\frac{\partial d_{G_1G_2}}{\partial\theta_1} + d_{G_1G_2}l\,\tan\, i_1'\,\cos\,\theta_1 = 0. \tag{10}$$

Meanwhile, Eq. (10) can be expressed as a form of the vector triangle AB_2C_2. With $\overrightarrow{OB_2} - \overrightarrow{OB_1} = \overrightarrow{AB_2} - \overrightarrow{AB_1}$, as shown in Fig. 3,

$$\begin{cases} R_2\cos(\theta_2 + i_2') - R_2\cos(\theta_1 + i_1') = d'_{G_1G_2}\cos\theta_2 - d_{G_1G_2}\cos\theta_1 \\ R_2\sin(\theta_2 + i_2') - R_2\sin(\theta_1 + i_1') = d'_{G_1G_2}\sin\theta_2 - d_{G_1G_2}\sin\theta_1 \end{cases}. \tag{11}$$

By differentiating Eq. (11) with respect to θ_1, we obtain

$$\frac{\partial d_{G_1G_2}}{\partial\theta_1} = -d_{G_1G_2}\,\tan\, i_1'. \tag{12}$$

Moreover, Eq. (10) defines the optimal value of $d_{G_1G_2}$ for astigmatism correction in the working waveband, which

Downloaded From: http://opticalengineering.spiedigitallibrary.org/ on 05/29/2016 Terms of Use: http://spiedigitallibrary.org/ss/TermsOfUse.aspx

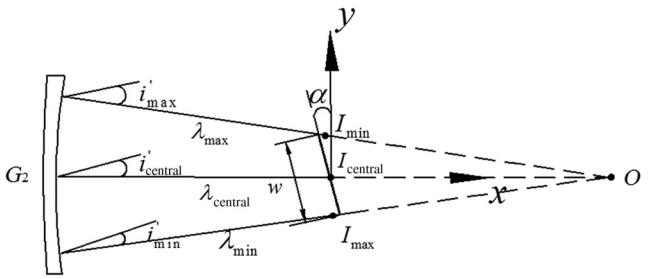

Fig. 3 Optical layout of the imaging plane. The width of the working band ranges from λ_{min} *to* λ_{max}. i' is the inclined angle for G_2 at different wavelengths. w is the width of the imaging plane between 2 wavelengths. O is the center of the Rowland circle of G_2.

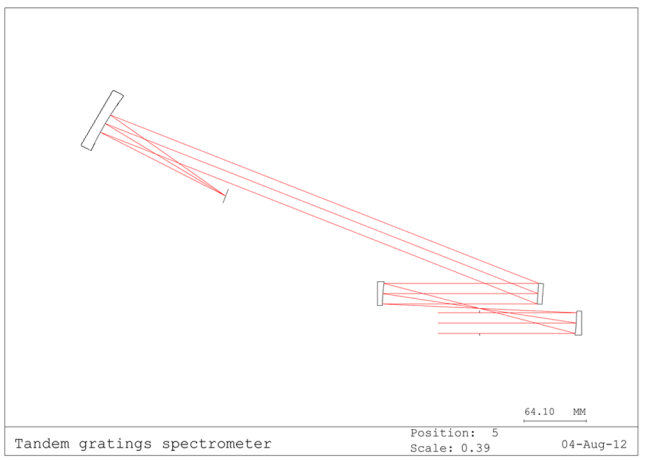

Fig. 4 Optical layout of the modified tandem gratings spectrometer.

Table 1 Specifications, design parameters, and performances for the modified tandem gratings spectrometer.

Specifications	Spectral coverage	280–360 nm
	Spatial pixel resolution	<0.26 mrad
	Spectral resolution	<0.167 nm
	F#/number	7
Parameters of design	Front optical system	Concentric off-axis Parabolic mirrors with radius 200 mm
	Field of view	1.6 deg×0.01 deg
	Slit	3 mm × 0.02 mm
	Plane grating	Ruling density 700 line/mm incident angle 3.95 deg
	Concave grating	Ruling density 600 line/mm inclined angle 11.07 deg with radius 300 mm
	$d_{G_1G_2}$	487.30 mm
	d_{G_1I}	151.41 mm
	α	2.73 deg
Performances	RMS spot radii	3.7 – 25.7 μm
	MTF at 20 lp/mm	>0.5

simultaneously determines the best focal distance suitable for each wavelength. The result of Eq. (10) is

$$d_{G_1G_2} = R_2 \cos i'_1 \left(\frac{\tan i'_1}{\tan \theta_1} + 1 \right). \tag{13}$$

As shown in Fig. 2, the spectral resolution is expressed as follows:

$$d\lambda = \frac{d\theta_1}{dw} \cdot \frac{d\lambda}{d\theta_1} \cdot dw, \tag{14}$$

where, $d\lambda/d\theta_1 = mg_1/\cos\theta_1$ is the angular dispersion of G_1, m is the given diffraction order ($m = 1$), and w is the width of the imaging plane of 2 different wavelengths. The corresponding minimal value of dw is written as

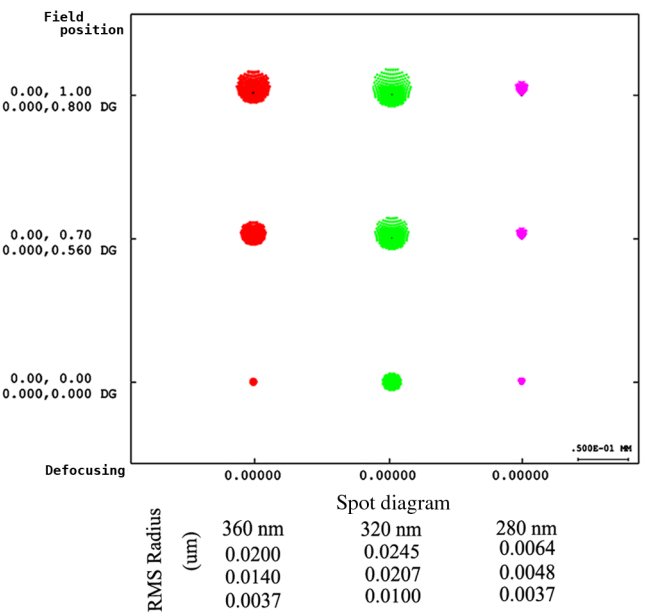

Fig. 5 The root mean square (RMS) spot diagram at different wavelengths.

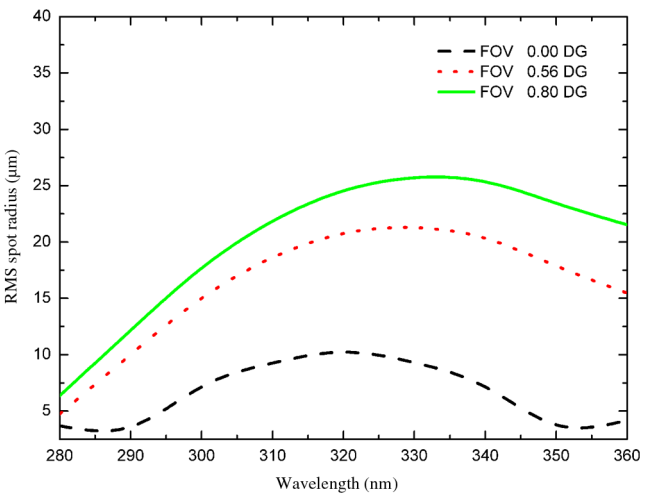

Fig. 6 RMS spot radius versus wavelength of the modified tandem gratings spectrometer.

Downloaded From: http://opticalengineering.spiedigitallibrary.org/ on 05/29/2016 Terms of Use: http://spiedigitallibrary.org/ss/TermsOfUse.aspx

$$dw = \frac{s \cos i_1 \cos i_1'}{f_1 \cos \theta_1 \cos \theta_1'} \cdot \frac{f_2}{\cos \alpha}. \tag{15}$$

According to the optimal Wadsworth condition, $\theta_1' = 0$. f_1 and f_2 are the focal lengths of front optical system and G_2. s is the width of slit and α is the inclined angle of the imaging plane. It is also the minimal spectral bandwidth that the imaging spectrometer can distinguish on the imaging plane (the width of slit imaging).

The imaging plane satisfies the parabola equation. According to Wadsworth condition, the rays of diffraction of G_2 focus on the center of its Rowland circle. As shown in Fig. 4, the inclined angle α is estimated as follows:

$$\alpha \approx \arcsin \frac{OI_{\text{central}} - OI_{\text{min}}}{w/2}. \tag{16}$$

From Eq. (3), Wadsworth condition and the basic grating equation, we obtain

$$\begin{cases} OI = R_2 \cos i'(1 + \cos i')^{-1} \\ g\lambda = \sin i' \end{cases}. \tag{17}$$

Then the inclined angle α can be expressed as follows:

$$\alpha = \arcsin\left(\frac{2R_2}{w}\left\{\left[1 + \sqrt{1 - (g\lambda_{\text{central}})^2}\right]^{-1} - \left[1 + \sqrt{1 - (g\lambda_{\text{min}})^2}\right]^{-1}\right\}\right). \tag{18}$$

For vector triangles AB_1M_1, AB_2M_2 and AI_1I_2:

$$\begin{cases} w \sin(\theta_1 + i_1') = d_{G_2I_2} \cos(\theta_2 + i_2') - d_{G_2I_1} \cos(\theta_1 + i_1') + d'_{G_1G_2} \cos \theta_2 - d_{G_1G_2} \cos \theta_1 \\ w \cos(\theta_1 + i_1') = d_{G_2I_2} \sin(\theta_2 + i_2') - d_{G_2I_1} \sin(\theta_1 + i_1') - d'_{G_1G_2} \sin \theta_2 + d_{G_1G_2} \sin \theta_1 \end{cases}. \tag{19}$$

It is differentiated with respect to θ_1 and the evaluated expression is

$$\frac{dw}{d\theta_1} = \frac{(R_2 \cos i_1' + l \cos \theta_1)[1 + \cos i_1' + \cos 2(i_1' + \theta_1)]}{\cos i_1'(1 + \cos i_1')}. \tag{20}$$

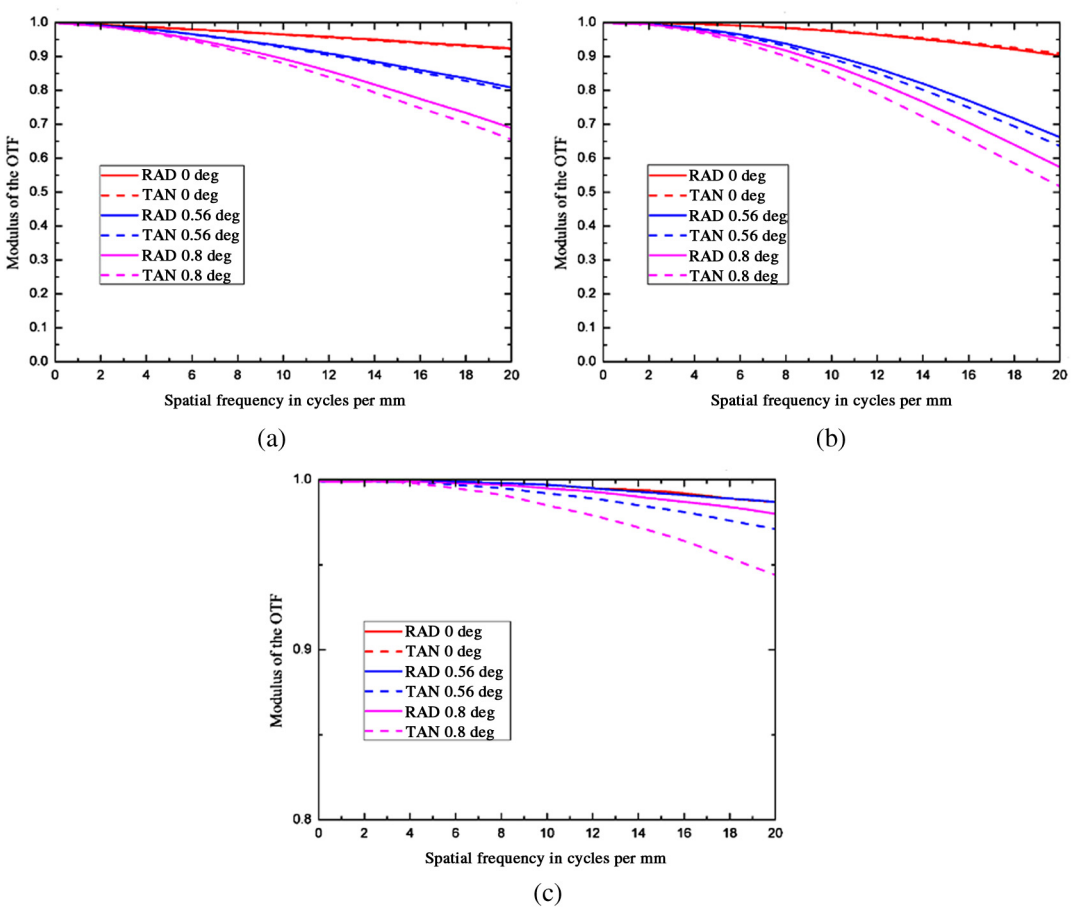

Fig. 7 Modulation transfer function (MTF) curve versus spatial frequency at different wavelengths of modified tandem gratings spectrometer with oblique incidence: (a) 360, (b) 320, and (c) 280 nm (color online).

Downloaded From: http://opticalengineering.spiedigitallibrary.org/ on 05/29/2016 Terms of Use: http://spiedigitallibrary.org/ss/TermsOfUse.aspx

In vector triangle OI_1I_2:

$$\begin{cases} w = I_1I_2 = (OI_1^2 + OI_2^2 - \angle I_1OI_2)^{\frac{1}{2}} \\ OI = R_2 - (R_2/1 + \cos\ i') \\ \angle I_1OI_2 = (\theta_2 + i_{2'}) - (\theta_1 + i_{1'}) \end{cases}. \tag{21}$$

Therefore, the spectral resolution can be expressed as

$$d\lambda = \frac{\cos i_1 \cos i_1'(1+\cos i_1')}{R_2(1+\tan i_1'/\tan\theta_1)[1+\cos i_1' + \cos 2(i_1'+\theta_1)]\cos\alpha} \cdot \frac{sf_2}{mg_1f_1}. \tag{22}$$

3 Design Procedure

A modified tandem gratings spectrometer with bandwidth ranging from 280 to 360 nm is designed using the CODE V software in this paper. The optical layout of this spectrometer is shown in Fig. 4, while its specifications and performances are listed in Table 1. A charge-coupled device (CCD) with a size of 13.3 mm × 13.3 mm (pixel size 26 μm × 26 μm, pixel number 512 × 512) is chosen in this study. The optimized system has spot size less than 26 μm, as shown in Fig. 5. To show the result of the aberration correction for broadband spectral simultaneity, the root mean square (RMS) spot radius is given as a function of the wavelength for the modified tandem gratings spectrometer, as shown in Fig. 6. The RMS spot radius is less than 25.7 μm in broadband spectral, and can be enclosed in a square pixel of 26 μm. The modulation transfer function (MTF) curves are given as a function of spatial frequency in Fig. 7. It is clear that the MTF of each field is larger than 0.5 at the Nyquist frequency (20 line pairs/mm) of the CCD for central and marginal wavelengths.

Spatial and spectral uniformity are essential properties of imaging spectrometers. Typical distortion requirements go down to 20% or even 10% of a pixel for an accurate

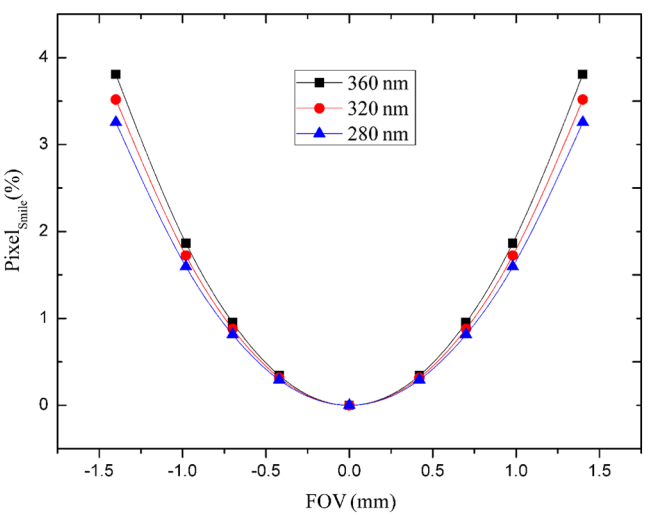

Fig. 8 Total smile for different wavelengths.

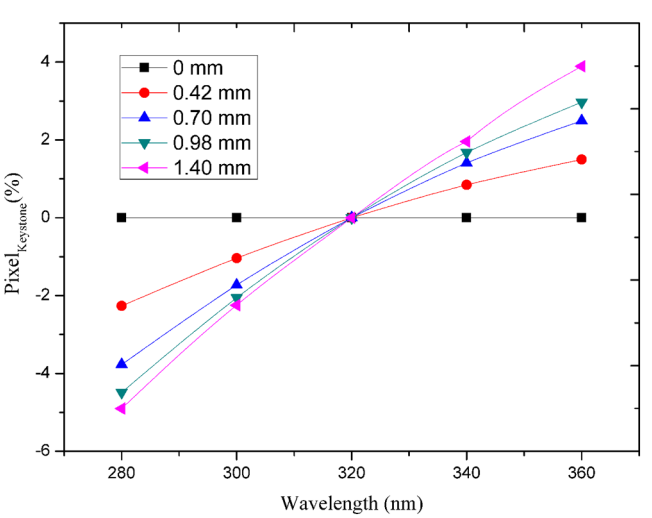

Fig. 9 Keystone for different object heights.

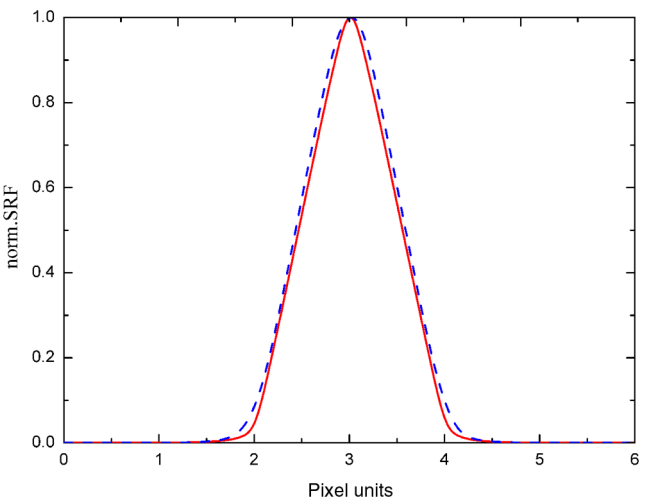

Fig. 10 Maximum spectral response function (SRF) variation of tandem gratings spectrometer. The 2 curves represent SRFs from 2 different field positions at a single wavelength. The wavelength and field positions were chosen to represent the worst case (maximum difference) for all wavelengths and fields.

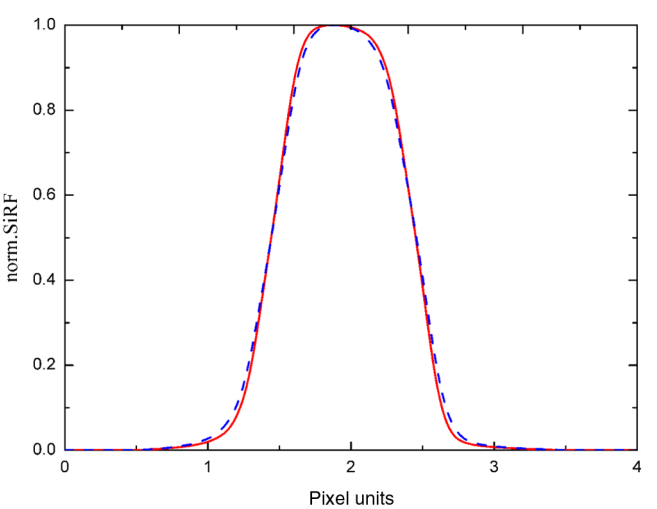

Fig. 11 Maximum spatial response function (SiRF) variation of tandem gratings spectrometer. The 2 curves represent SiRFs for 2 different wavelengths at a single field position. The wavelength and field positions were chosen to represent the worst case (maximum difference) for all wavelengths and fields.

Downloaded From: http://opticalengineering.spiedigitallibrary.org/ on 05/29/2016 Terms of Use: http://spiedigitallibrary.org/ss/TermsOfUse.aspx

acquisition of hyperspectral data. The total smile for different wavelengths is shown in Fig. 8. The total smile is symmetrical around the center of slit, and increases with the wavelengths. However, the total smile is less than 4% of a pixel. As shown in Fig. 9, the keystone is increased when the object height is higher. For a single height, the keystone of the marginal wavelength is larger than central wavelength. The keystone is approximately ±4% of a pixel. The result demonstrates that good imaging quality is obtained over the broad wavelength region by the modified spectrometer with tandem gratings and oblique incidence, and the results satisfy the application requirement of the design.

Besides, good spatial and spectral coregistration is also important criteria for the image quality of imaging spectrometer. Spatial misregistration, caused by keystone and variations in the point spread function (PSF) across the spectral channels, distorts the captured spectra.[13] Meanwhile, a similar error occurs in the spectral direction (spectral misregistration, caused by smile and corresponding PSF variations). In order to evaluate the variations in PSF, the maximum variation of spectral response function (SRF) and spatial response function (SiRF) is considered in this paper,[14] as shown in Figs. 10 and 11. It can be seen that there is a small variation of SRF (~4% in terms of half width), and the SiRF half-width variation is ~2% in our design. Then the MTFs of different wavelengths are similar enough to ensure good spatial coregistration.

A modified tandem gratings spectrometer with oblique incidence is proposed and designed in this paper. Through geometric analysis, the structure and spectral resolution of the modified tandem gratings spectrometer are determined. Under the same high spectral resolution, F-number and field of view, the lowest MTF of Offner spectrometer is worse than that of tandem gratings spectrometer at max, min, and central wavelengths, as shown in Table 2. The MTF curve of Offner spectrometer is shown in Fig. 12.

Table 2 The lowest modulation transfer function (MTF) of tandem gratings spectrometer and Offner spectrometer.

Wavelength (nm)	360	320	280
Tandem gratings spectrometer	0.655	0.517	0.944
Offner spectrometer	0.642	0.407	0.778

4 Conclusions

We present a modified tandem gratings spectrometer with high spectral resolution, along with the different ruling densities of the tandem gratings, and astigmatism correction in spectral broadband. Besides, the central light from the foreoptics is oblique incident on the spectrometer, which allows flexibility in selecting the types of gratings, and the grating of tandem gratings spectrometer is not going to be sensitive to polarization of the incoming light. The designed method

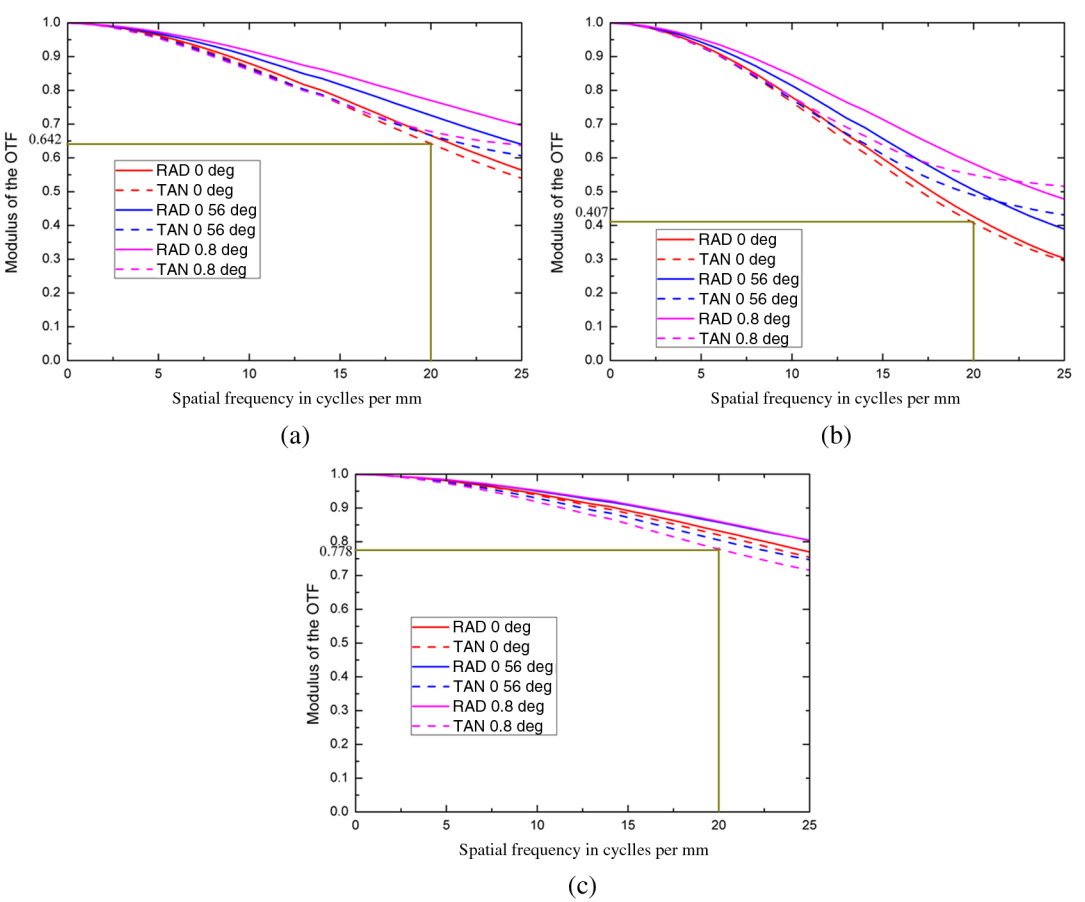

Fig. 12 MTF curve of Offner spectrometer versus spatial frequency with different wavelength: (a) 360, (b) 320, and (c) 280 nm (color online).

Downloaded From: http://opticalengineering.spiedigitallibrary.org/ on 05/29/2016 Terms of Use: http://spiedigitallibrary.org/ss/TermsOfUse.aspx

for correcting astigmatism is developed based on geometric aberration theory and Wadsworth condition. The anastigmatic imaging condition and the parameters of tandems gratings spectrometer are also determined. Compared with the concentric systems, such as the Offner and Dyson imaging spectrometers, our design is suitable for UV and visible–infrared remote sensing with high spectral resolution. An example for the UV band (280–360 nm) is provided to verify the optical performance of the design in this paper.

Acknowledgments

The research reported in this paper is supported by the National Natural Science Foundation of China (NSFC) under Grant No. 41105014.

References

1. X. Prieto-Blanco et al., "The Offner imaging spectrometer in quadrature," *Opt. Express* **18**, 12756–12769 (2010).
2. Q. Xue, "Modified Schwarzschild imaging spectrometer with a low F-number and a long slit," *Appl. Opt.* **52**, 6956–6961 (2013).
3. L. Guanter et al., "Scene-based spectral calibration assessment of high spectral resolution imaging spectrometers," *Opt. Express* **17**, 11594–11606 (2009).
4. P. Mouroulis, R. O. Green, and D. W. Wilson, "Optical design of a coastal ocean imaging spectrometer," *Opt. Express* **16**, 9087–9096 (2008).
5. J. Liu, W. H. Fan, and L. C. Chen, "Route of delivering 40-fs ultrashort laser pulses for gating photoconductive antenna in fiber-coupled terahertz time-domain spectroscopy," *Opt. Eng.* **51**, 085001 (2012).
6. K. S. Lee, K. P. Thompson, and J. P. Rolland, "Broadband astigmatism-corrected Czerny–Turner spectrometer," *Opt. Express* **18**, 23378 (2010).
7. M. Beasley et al., "Imaging spectrograph for interstellar shocks: a narrowband imaging payload for the far ultraviolet," *Appl. Opt.* **43**, 4633 (2004).
8. P. Lemaire. "Ultraviolet conical diffraction: a near-stigmatic tandem grating mounting spectrometer," *Appl. Opt.* **30**, 1294–1302 (1991).
9. X. Prieto-Blanco et al., "Analytical design of an Offner imaging spectrometer," *Opt. Express* **14**, 9156–9168 (2006).
10. J. D. F. Bartoe and G. E. Brueckner, "New stigmatic, coma-free, concave-grating spectrograph," *J. Opt. Soc. Am.* **65**, 13 (1975).
11. L. Yu and G. Lin, "Advanced astigmatism-corrected tandem Wadsworth mounting for small-scale spectral broadband imaging spectrometer," *Appl. Opt.* **52**, 82–89 (2013).
12. H. Beutler, "The theory of concave grating," *J. Opt. Soc. Am.* **35**, 311–350 (1945).
13. G. Høye, T. Løke, and A. Fridman, "Method for quantifying image quality in push-broom hyperspectral cameras," *Opt. Eng.* **54**(5), 053102 (2015)
14. P. Mouroulis, R. O. Green, and T. G. Chrien, "Design of pushbroom imaging spectrometers for optimum recovery of spectroscopic and spatial information," *Appl. Opt.* **39**(13), 2210–2220 (2000)

Chengguang Cui is a PhD candidate of optical engineering at Changchun Institute of Optics, Fine Mechanics and Physics, Chinese Academy of Sciences. He received his BS degree from Nankai University and B.B.A from Tianjin University. His current research interests include hyperspectral imaging, radiation calibration, and spacecraft simulation in Satellite Tool Kit.

Shurong Wang is a senior research scientist at Changchun Institute of Optics, Fine Mechanics and Physics, Chinese Academy of Sciences. She has been working in State Key Laboratory of Applied Optics since 1986. Her current research interests include space ultraviolet remote sensing techniques and radiation calibration.

Yu Huang is a researcher at Changchun Institute of Optics, Fine Mechanics and Physics, Chinese Academy of Sciences, where he received his PhD in optical engineering in 2007. His current research interests include space ultraviolet remote sensing techniques and radiation calibration.

Qingsheng Xue is an optical designer at Changchun Institute of Optics, Fine Mechanics and Physics, Chinese Academy of Sciences. He received his PhD in optical engineering in 2010 at the State Key Laboratory of Applied Optics. In addition to his main optical design activities, his interests include optical test.

Bo Li is a researcher at Changchun Institute of Optics, Fine Mechanics and Physics, Chinese Academy of Sciences, since he received his PhD in optical engineering in 2011. His current research interests include optical design, optical detection, and radiation calibration.

Lei Yu is a optical designer at Changchun Institute of Optics, Fine Mechanics and Physics, Chinese Academy of Sciences, where he received his PhD in optical engineering in 2012.

Downloaded From: http://opticalengineering.spiedigitallibrary.org/ on 05/29/2016 Terms of Use: http://spiedigitallibrary.org/ss/TermsOfUse.aspx